Monatshefte für Chemie 133, 773–784 (2002)

Monatshefte für Chemie
Chemical Monthly

Preparation of Nanostructured Magnetic Films by the Plasma Jet Technique

Frantisek Fendrych[1,*], **Ludek Kraus**[1], **Oleksandr Chayka**[1], **Peter Lobotka**[2], **Ivo Vavra**[2], **Jan Tous**[1], **Vaclav Studnicka**[1], and **Zdenek Frait**[1]

[1] Institute of Physics, ASCR, CZ-18221 Praha 8, Czech Republic
[2] Institute of Electrical Engineering, SAS, SK-84239 Bratislava, Slovak Republic

Summary. Magnetic films were prepared by the plasma jet technique from Fe, mumetal, and Fe/Hf or Fe/Ta nozzles. Two different plasma jet systems with different vacuum pumps were used to compare the quality of the produced films. The films prepared from a Fe nozzle in the two different equipments shows that oxygen in the residual atmosphere of the low vacuum reactor leads mainly to the formation of iron oxides. The Fe and mumetal films prepared in the high vacuum system contain only a very small amount of oxygen, as proved by chemical analysis and ferromagnetic resonance. The mumetal film, moreover, shows good soft magnetic properties and low magnetic damping. For the reactive plasma jet deposition of nanogranular Fe–Hf–O and Fe–Ta–O films, the low vacuum system was used. The films with higher oxygen content exhibit tunneling-type conductivity. In some films, superparamagnetic behaviour and spin-dependent tunneling magnetoresistance were observed.

Keywords. Plasma jet; Magnetic films; Nanogranular materials; Tunneling magnetoresistance.

Introduction

Magnetic films are nowadays very important, both from technical application and basic research points of view. A large variety of methods is being used to produce magnetic films. For the new applications, however, new magnetic materials and also new deposition techniques are required. The plasma jet technique described below has only recently been used for the preparation of magnetic films [1–4].

The plasma jet technique was developed in the Institute of Physics, Czechoslovak Academy of Sciences [5]. The principle of the method is schematically shown in Fig. 1. The material to be deposited originates from the nozzle, which is sputtered by the ions produced in the hollow cathode discharge generated inside the nozzle. In the basic configuration the plasma jet reactor consists of two electrodes: the grounded walls of the reactor (anode) and the water-cooled cylindrical nozzle (cathode) which is connected to the DC or radio frequency power source. The substrate is placed on the electrode, which can be grounded or biased with respect to the ground potential. The working gas (or mixture of gases) enters

* Corresponding author. E-mail: fendrych@fzu.cz

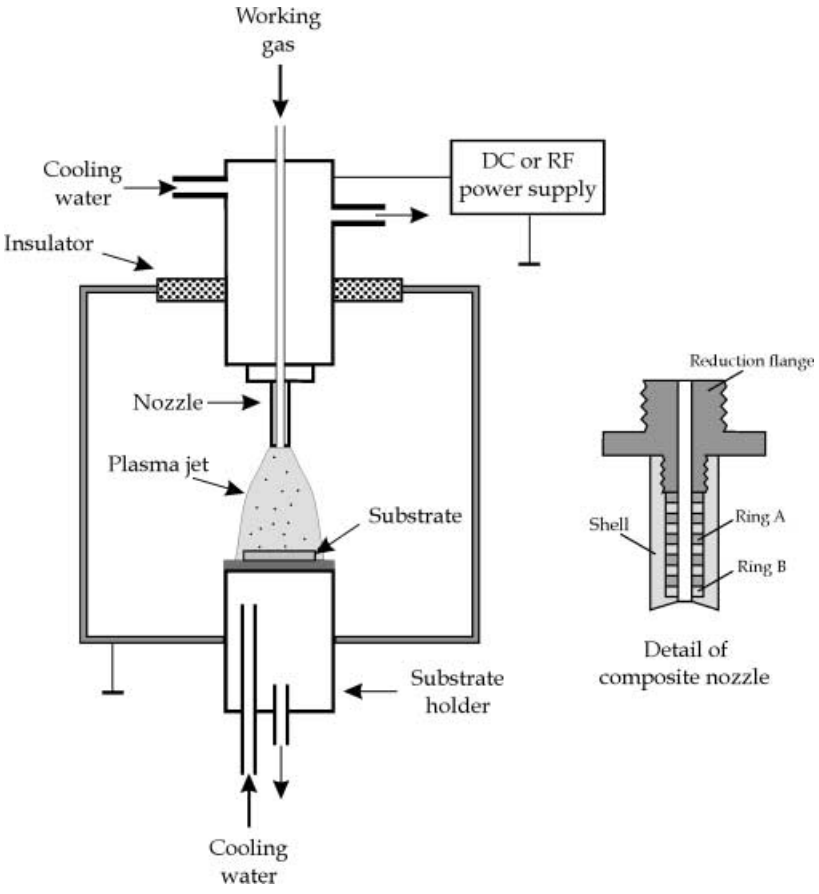

Fig. 1. Schematic view of plasma jet reactor

the reactor through the nozzle and is continuously pumped by the vacuum system. The pressure in the reactor chamber is maintained at several tens of Pa. The flow of working gas and the pumping speed can be adjusted so that the velocity of gas at the outlet of the nozzle is supersonic. If the power fed to the nozzle exceeds a certain limit (for example, 20 W), an intensive hollow cathode discharge is generated inside the nozzle. Due to the bombardment by the ions produced in the discharge, the material of nozzle mouth is sputtered and enters the plasma. The working gas forces the discharge supersonically out of the nozzle, and a well-defined plasma jet superimposed on the primary plasma channel is formed. The atoms, ions, and clusters are transported to the substrate placed in the stream of plasma, and a film consisting of the nozzle material is deposited. In case of reactive plasma jet deposition a gas reacting with the nozzle material is added to the working gas, and chemical compounds can be then produced. More details on the plasma jet reactor can be found in Refs. [6, 7]. The advantage of the plasma jet technique with respect to the commonly used magnetron sputtering is the high deposition rate (of the order 1 μm/h) which can be achieved even for soft magnetic materials.

The plasma jet method has been successfully used for the preparation of various materials. Typical examples are the depositions of germanium nitride [8],

cooper nitride [9], and titanium nitride [10] thin films of defined stoichiometry, composite SiGe [11], *a*-Si:H [12], hard amorphous carbon nitride coatings [13, 14], *etc.*

Results and Discussion

Fe films

The films prepared from a single Fe nozzle in the two different plasma jet equipments differ substantially. Chemical analysis showed that the films prepared in the low-vacuum reactor contained large amounts of oxygen. The film composition as a function of position, measured along the line passing the center of plasma channel, is shown in Fig. 2. Three films prepared under identical conditions but with different working gas are compared. As can be seen, the oxygen content does not depend on the purity of the working gas. That means that the oxygen in the film originates from the residual atmosphere in the reactor. Its amount could not be reduced below 30 at.% even if the reactor was pumped for one week before the deposition. To reduce the oxygen content in the films, some H_2 was added to the Ar. This leads to a substantial reduction of oxygen in a small circular spot around the plasma channel axis. Further from the substrate center, even higher oxidation of the film is observed. The quality of the film within the spot is rather poor with very small adhesion. X-Ray diffractions of these films indicate the presence of Fe oxides. Only weak traces of metallic Fe can be found in the films prepared in an Ar/H_2 atmosphere. No FMR signal can be observed from films prepared with Ar only; the film prepared in Ar/H_2 has not been measured because of its poor quality.

The films deposited in the high-vacuum reactor from the Fe nozzle on Si substrates show metallic luster and good adhesion to the substrate. Chemical analysis reveals only little contamination by oxygen (less than 6 at.%). The FMR measured with the magnetic field parallel to the film plane is shown in Fig. 3. In the

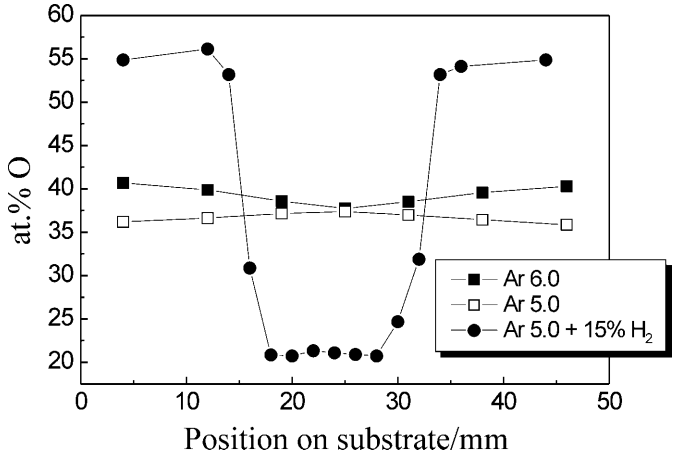

Fig. 2. Oxygen content in Fe-films prepared in the low-vacuum reactor with different working gas atmosphere

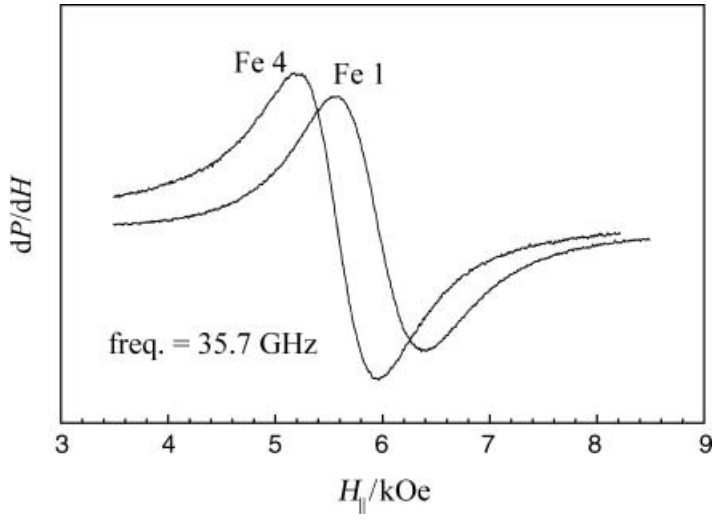

Fig. 3. Ferromagnetic resonance on Fe films deposited in the high-vacuum reactor

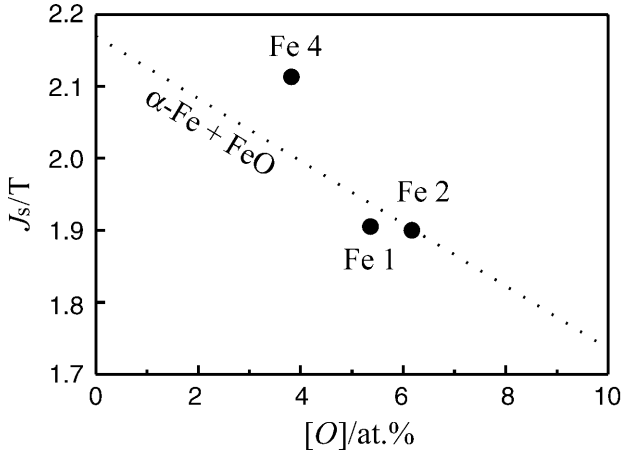

Fig. 4. Saturation polarization J_s of Fe + FeO samples as a function of the oxygen content

perpendicular configuration the resonance fields exceed the maximum field available with our electromagnet. The saturation polarization J_s calculated from *Kittel*'s resonance condition for an isotropic film with $g = 2.09$ [15] is shown in Fig. 4 as a function of the oxygen content. The dotted line represents the saturation polarization of a mixture of α-Fe and the nonmagnetic oxide FeO. As can be seen, the value $J_s = 2.11$ T for the film Fe 4 is very close to the value of 2.17 T for the bulk Fe. Figure 5 shows the hysteresis loop of the film. The rather high coercive force (about 3 kA/m) indicates that the film is polycrystalline.

Mumetal films

The mumetal films were prepared in the high-vacuum apparatus from the PY 79M nozzle. The films were deposited either on glass or Si substrates.

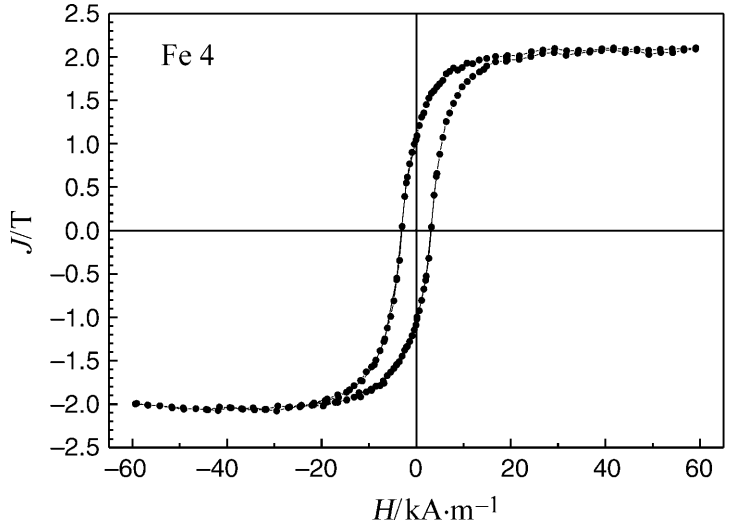

Fig. 5. Hysteresis loop of Fe film deposited in the high-vacuum plasma jet reactor

Electron probe microanalysis showed that the film stoichiometry did not differ by more than 2 at.% from the nozzle composition and that the increase of oxygen content with respect to the nozzle material was less than 0.4 at.% (in the bulk material, 1.8 at.% O were detected). X-ray diffraction pattern of the film on Pyrex glass shows diffraction peaks typical for an fcc-cubic structure with a lattice constant of $a = 3.554$ Å.

The results of ferromagnetic resonance measurements at 35.7 GHz with the magnetic field applied parallel and perpendicular to the film are shown in Fig. 6.

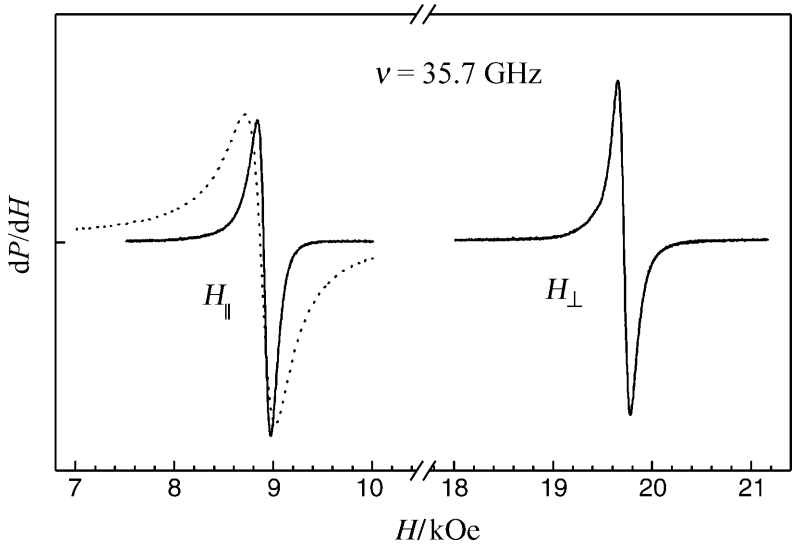

Fig. 6. Ferromagnetic resonance of a mumetal film measured with magnetic field parallel ($H_{\|}$) and perpendicular ($H_{\perp}$) to the film plane; FMR of the original bulk tape is shown by the dotted curve

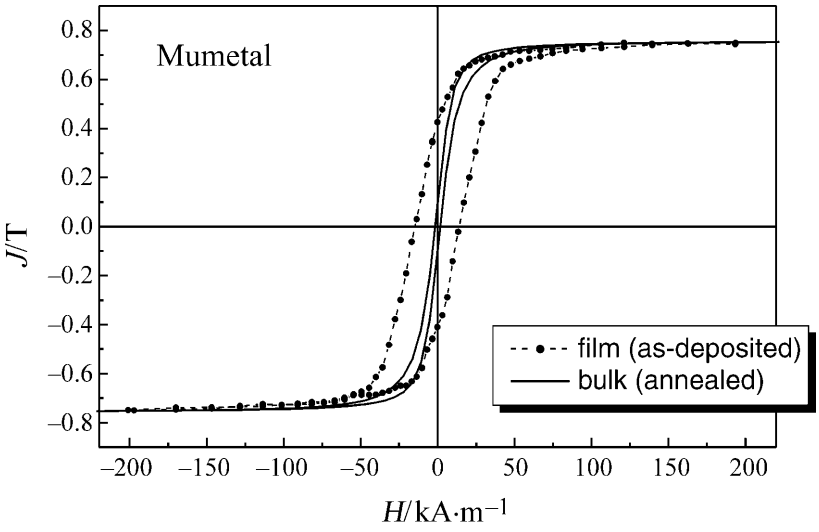

Fig. 7. Hysteresis loops of the mumetal film and the bulk mumetal tape

For comparison, the parallel resonance of the original PY 79M tape is also shown. From *Kittel*'s resonance condition for an isotropic film, the spectroscopic splitting factor $g = 2.108$ and the saturation polarization $J_s = 0.77\,\mathrm{T}$ are obtained. This J_s value is identical with J_s of the original bulk alloy obtained from the hysteresis loop measurement-another proof that only very little oxygen is present in the μ-metal film. The FMR linewidth measurements at two different microwave frequencies (35.7 and 69 GHz) yield the intrinsic *Landau-Lifshitz* relaxation constant as $1.04 \times 10^8\,\mathrm{rad/s}$, in good agreement with values for 80/20 permalloy ($\sim 8 \times 10^7\,\mathrm{rad/s}$) films [16]. The low value of relaxation constant indicates a good quality of the plasma deposited film.

In Fig. 7, the hysteresis loop of the film is compared with the loop of a bulk tape (0.05 mm thick, 3 mm wide) made of the same material. The coercive force 14 A/m of the film is about one order of magnitude higher than $H_c = 1.6\,\mathrm{A/m}$ of the optimally annealed tape, but it is much smaller than $H_c = 365\,\mathrm{A/m}$ of the rolled tape. This result illustrates that good soft magnetic films can be produced by plasma jet deposition in the high-vacuum equipment.

Fe–Hf–O and Fe–Ta–O films

Nanogranular magnetic films consisting of tiny metallic grains in a nonmetallic matrix exhibit interesting magnetic and electron transport properties [17]. Many combinations of metal and nonmetal materials have been investigated (see *e.g.* Ref. [18]). Recently, such films were prepared mostly by the reactive sputtering from metallic targets in a mixed Ar and O_2 (or N_2) atmosphere. For example, if a ferromagnetic metal (Fe, Co, or Ni) is sputtered together with an inmiscible element which has a large affinity to oxygen (or nitrogen), the ferromagnetic metal can precipitate into small crystalline grains surrounded by the oxide or nitride matrix of the other element. We tried to prepare Fe-based nanocomposite films in the low-vacuum plasma jet reactor.

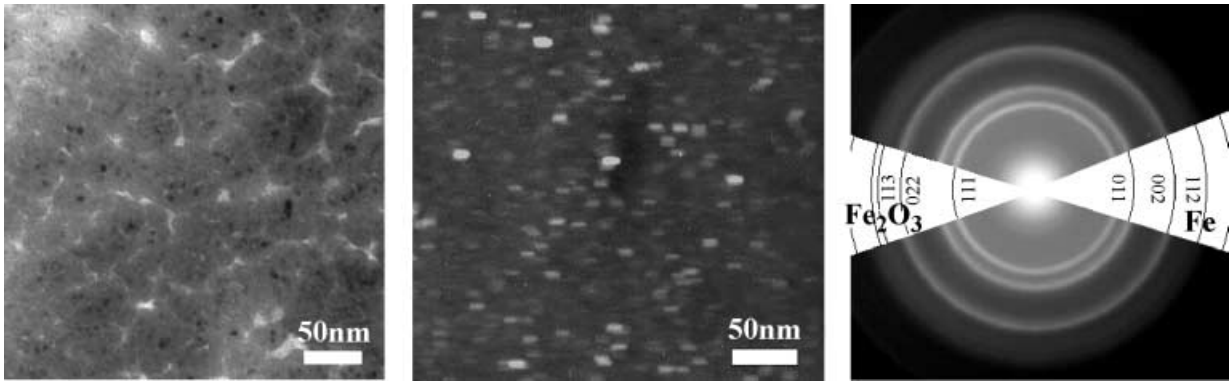

Fig. 8. TEM micrographs and electron diffraction of a nanogranular $Fe_{33.7}Ta_{9.5}O_{56.8}$ film; a) bright field image, b) dark field image, c) selective area diffraction

Because the partial pressure of oxygen in the low-vacuum reactor is rather high, O_2 need not be added to Ar to obtain the oxides of Hf or Ta. Moreover, sometimes hydrogen had to be added to Ar to prevent the oxidation even of the ferromagnetic metal. The Fe–Hf–O and Fe–Ta–O films prepared from the composite nozzles were investigated systematically [1–4]. Some of them really exhibit a nanogranular structure as shown by electron transmission microscopy (Fig. 8a,b). Bcc–Fe grains with a grain size of few nm can be found in an amorphous matrix. The electron diffraction revealed also some traces of crystalline Fe_3O_3 (Fig. 8c). It means that the surface of the bcc–Fe nanocrystals is probably oxidized. X-Ray diffraction of such films shows only a broad weak diffraction peak near the [110] reflection of bcc–Fe on an amorphous background. This fact is in correlation with TEM investigations because of the lower sensitivity of X-ray diffraction analysis.

Magnetic and electric properties of the films depend on the content of oxygen and on the Hf/Fe (or Ta/Fe) ratio. Ferromagnetic resonance measurements on Fe–Ta–O films revealed superparamagnetic behaviour, characterized by broad resonance peaks near the paramagnetic resonance field, for the compositions with a Ta/Fe ratio close to 0.25 [3].

The electrical resistivity ρ and its temperature dependence are very sensitive to the oxygen concentration. A large increase of ρ (by about 6 orders of magnitude) is observed for a content of above 50 at.% O. The temperature dependence of resistivity changes from the typical metallic behaviour at low O content to $\ln\rho \propto T^{1/2}$ for high O concentration (Fig. 9). Such a dependence is characteristic for the electron tunneling in metal/insulator granular systems [19]. The tunneling type of conductivity can be also proved by the dependence of differential conductance, $G = \mathrm{d}I/\mathrm{d}V$, on the bias voltage V. An example for a nanogranular Fe–Ta–O film is shown in Fig. 10. The fit of experimental data to the theoretical dependence $G \propto V^{1/2}$, typical for the inelastic tunneling of electrons through the non-metallic barrier [20], is shown by the dotted line.

In the films with tunneling type of conductivity and superparamagnetic behaviour, a high magnetoresistance (MR) was observed. An example can be seen in Fig. 11, where the MR of a film prepared from a Fe/Hf nozzle with a stainless

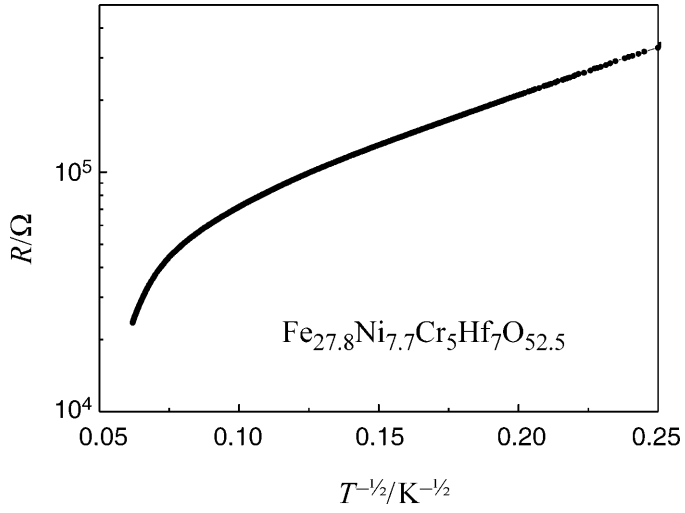

Fig. 9. Temperature dependence of resistivity of a nanogranular $Fe_{27.8}Ni_{7.7}Cr_5Hf_7O_{52.5}$ film

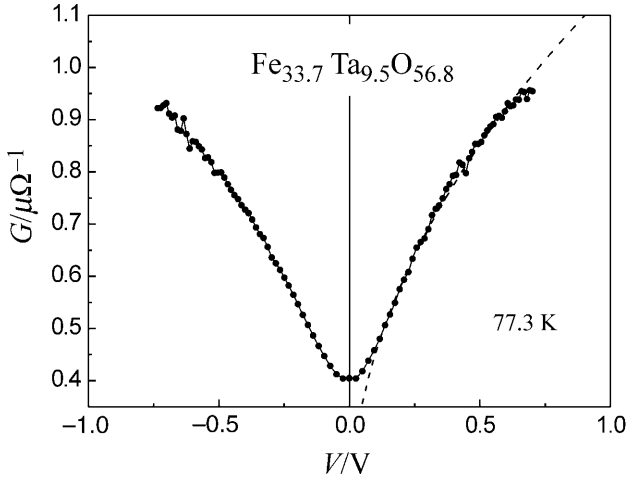

Fig. 10. Dependence of differential conductance $G = dI/dV$ on the bias voltage measured for a nanogranular Fe–Ta–O film at liquid nitrogen temperature

steel shell tube is shown. The magnetoresistance is isotropic in the film plane and follows well the theoretical dependence $\Delta\rho/\rho \sim -M^2$ [21]. The *m-H* curves, measured with the SQUID magnetometer at three different temperatures, are shown in the lower part of Fig. 11. In spite of similar magnetizing curves observed at 77.3 K and 300 K, the magnitudes of MR measured at these temperatures are very different. The enhancement of MR at lower temperature can be explained by higher-order spin-dependent tunneling [22]. We have tested this explanation by fitting the experimental curve R(V) measured at 77.3 K by the formula suggested in Ref. [22]. The result is shown in Fig. 12; a good agreement with the theoretical curve is evident. The MR enhancement is achieved due to the fact that the

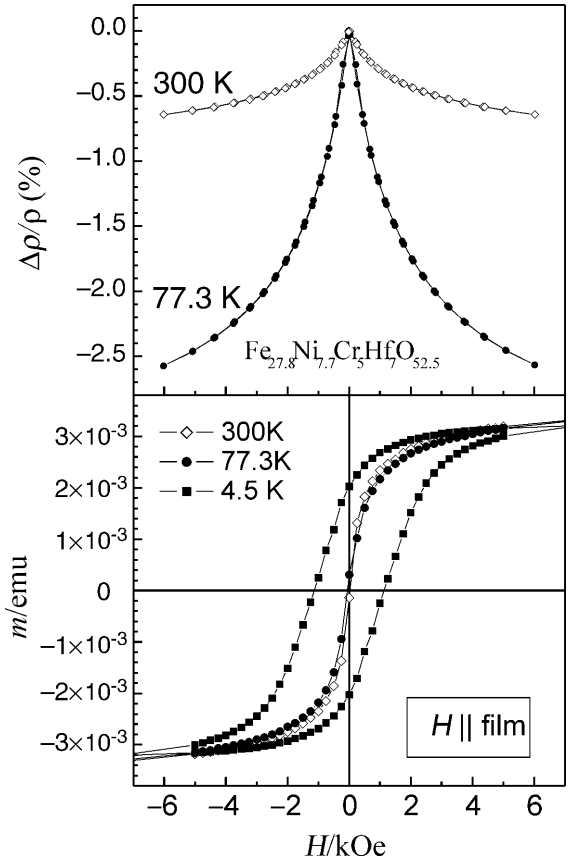

Fig. 11. Magnetoresistance (top) and the magnetizing curves (bottom) measured at different temperatures in a nanogranular $Fe_{27.8}Ni_{7.7}Cr_5Hf_7O_{52.5}$ film

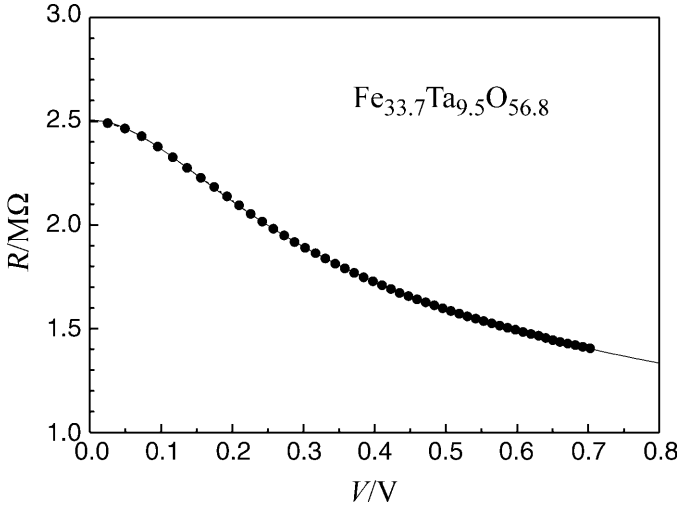

Fig. 12. Fit of the experimental dependence of the Fe–Ta–O film resistance R on the bias voltage V measured at 77.3 K; the fitting formula $R(V) = a(1 + bV^2)^{-C}$ was proposed by Mitani et al. in Ref. [22] assuming higher-order spin-dependent tunneling in granular systems when several electrons placed at neighboring granules tunnel simultaneously between them

probability of the higher-order tunneling is given by the product of probabilities of single tunneling events.

Conclusions

For the first time the supersonic plasma jet method has been used for deposition of magnetic films. It was proved that the quality of film sensitively depends on the vacuum system used for the pumping of the plasma reactor. The films deposited in the low vacuum reactor are highly contaminated by oxygen from the residual atmosphere. This system has been used for reactive deposition of nanogranular magnetic films consisting of Fe crystallites embedded in an oxide matrix. Some of these films exhibited spin-dependent tunneling magnetoresistance. The quality of the films prepared in the low vacuum reactor is, however, rather poor, and the chemical composition of films can be hardly controlled. To get high quality magnetic films with low (or well controlled) content of oxygen, the high-vacuum technology must be used for the plasma jet reactor.

Experimental

Two different plasma reactors were used for film preparation. The first (low vacuum) system uses a Roots vacuum pump and standard rubber seals. The limit pressure attainable in this reactor is about 5×10^{-2} Pa. An RF power supply (13.56 MHz) is used to generate the hollow cathode discharge in the nozzle. The single Fe nozzle (tube 3 cm long with inner and outer diameters of 3 and 6 mm, respectively) was used to test the system capability. Because the films prepared in this reactor are highly contaminated by the oxygen from the residual atmosphere, H_2 was added to the working gas (Ar) in order to reduce the oxygen content in some films. The low vacuum system was also used for the preparation of nanogranular magnetic films by reactive deposition. Deposition from two independent nozzles (Fe in combination with Hf or Ta) at 90° and 45° with respect to the substrate plane was attempted. The idea was to control the film composition by variation of the Fe and Hf (Ta) nozzle's distance from the substrate, by different flow rates of the working gas, or by a difference in the RF power supplied to the two nozzles. These films, however, were chemically very inhomogeneous, probably because the mixing of the two plasma channels was not ideal. To improve the film homogeneity, a single composite nozzle was used (for details see Fig. 1). The nozzle was composed of rings made of the two different metals (Fe and Hf or Fe and Ta) inserted in the outer (shell) tube. The number of Hf (or Ta) rings and their position with respect to the nozzle mouth were used to control the ratio of Hf/Fe (Ta/Fe) in the film. First, the reduction flange and the shell tube were made of stainless steel. Because these parts were also partially sputtered by the hollow cathode discharge, the films contained also Ni and Cr. To reduce the contamination of films by other elements, pure Fe was finally used for the reduction flange and the shell tube. These nanocomposite materials are generally thermodynamically metastable and have a tendency to relax at higher temperatures. To avoid grain growth and formation of stable phases in the developing films, the substrate holder was cooled by water.

The second (high vacuum) equipment was used to test whether high quality magnetic films can be prepared by the plasma jet technique. It uses a turbomolecular pump and copper vacuum seals. The limit pressure in this reactor is about 10^{-6} Pa. The substrate holder is not cooled. The DC hollow cathode discharge with plasma confined by a magnetic field was used for the deposition of Fe and μ-metal films. The same Fe nozzle as in the low vacuum system was used for Fe film deposition. The μ-metal films were prepared from a nozzle made of $Ni_{73}Fe_{15}Cu_7Mo_4Mn_1$ alloy. The mother alloy (commercial mark: PY 79M) was kindly supplied by Kovohute Rokycany, a.s.

The chemical composition of the films was studied by electron probe microanalysis on a JEOL Superprobe JXA-733 device equipped with an X-ray microanalyzer Kevex Delta class V. Two methods of analysis were used:

1. EDAX (energy dispersive analysis of characteristic X-ray radiation) using a multichannel semiconductor detector with a special beryllium window for light elements (up from boron).
2. WDAX (wave dispersive analysis of X-rays) using adjustable crystal spectrometers. A special multilayer crystal Ni–C (spacing: $2d = 84$ Å) was used as an X-ray diffraction mirror for the direct measurement of light elements (*e.g.* O, N). Pure samples of CuO and cubic BN were used as standards for O and N measurement, respectively.

First, the EDAX method was applied for the identification of chemical elements in the film and a rough estimation of their concentrations. WDAX was then utilized for the precise quantitative analysis of chemical elements identified by EDAX. In this way, an accuracy of chemical composition of about ± 0.1 wt.% was achieved.

The X-ray diffraction structure analysis was performed by means of a *Bragg-Brentano* focusation arrangement using CuK_α radiation. The magnetic properties were studied at room temperature by a computer controlled quasistatic hysteresis loop tracer. The saturation magnetization, g-factor, and magnetic relaxation parameter of the deposited films were determined from ferromagnetic resonance (FMR) at 36 and 69 GHz with the magnetic field applied parallel and perpendicular to the film plane. For the measurement of magnetization curves in nanogranular films the SQUID magnetometer (Quantum Design MPMS-5S) was used.

The resistance of low resistive samples (less than 200 MΩ) was measured by the four-terminal method using a conventional digital multimeter. For high resistive samples, the two-terminal method and an electrometer were used. For the resistance measurement the films were deposited on glass substrates. The electric contacts were prepared by electron gun deposition of Ag films either below or on the top of the investigated film. The electrical leads were glued to the Ag films by silver paint. The temperature dependence of resistivity was examined in the range of 4.2–300 K. The magnetoresistance at 77 K and room temperature was measured in an electromagnet with its magnetic field (up to 6 kOe) applied parallel or perpendicular to the film plane.

Acknowledgements

This work has been supported by the COST-523 European Concerted Action on Nanostructured Materials and by the Grant Agency of the Czech Academy of Sciences under Project No. A1010204. The paper was presented at the COST-523 Mid Term Meeting in Limerick, Ireland, October 4–6, 2001.

References

[1] Soyka V, Kraus L, Fendrych F, Sicha M, Hubicka Z, Frait Z, Jastrabik L (1999) 26th Int Conf on Metallurgical Coatings and Thin Films, April 12–15, 1999, San Diego, California, USA, Book of Abstracts, p 85
[2] Soyka V, Kraus L, Frait Z, Sicha M, Jastrabik L (2000) Acta Physica Polonica A **97**: 515
[3] Kraus L, Chayka O, Tous J, Fendrych F, Pirota KR, Sicha M, Jastrabik L (2001) Int Conf on Magnetism, August 6–11, 2000, Recife, Brazil; J Magn Magn Mater **226**–**230**: 669
[4] Kraus L, Chayka O, Fendrych F, Frait Z, Sicha M, Tous J (2000) 16th Int Conf on Magnetic Films and Surfaces, August 14–18, Natal, Brazil, Book of Abstracts, paper 15P24
[5] Bardos L, Vu NQ (1989) Czech J Phys B **39**: 731
[6] Novak M, Sicha M, Kapicka V, Jastrabik L, Soukup L, Hubicka Z, Klima M, Slavicek P, Brablec A (1997) Journal de Physique IV Coloque Suppl C4-331

[7] Hubicka Z, Pribil G, Soukup RJ, Ianno NJ (2002) Surface and Coatings Technology (submitted)
[8] Soukup L, Perina V, Jastrabik L, Sicha M, Pokorny P, Soukup RJ, Novak M, Zemek J (1996) Surface and Coatings Technology **78**: 280
[9] Fendrych F, Soukup L, Jastrabik L, Sicha M, Hubicka Z, Chvostova D, Tarasenko A, Studnicka V, Wagner T (1999) Diamond and Related Materials **8**: 1715
[10] Barankova H, Bardos L, Berg S (1995) J Electrochem Soc **142**: 883
[11] Sicha M, Hubicka Z, Soukup L, Jastrabik L, Cada M, Spatenka P (2001) Surface and Coatings Technology **148**: 199
[12] Pribil G, Hubicka Z, Soukup RJ, Ianno NJ (2001) J Vacuum Science Technol **A19(4)**: 1571
[13] Fendrych F, Pajasova L, Wagner T, Jastrabik L, Chvostova D, Soukup L, Rusnak K (1999) Diamond and Related Materials **8**: 1711
[14] Hubicka Z, Sicha M, Pajasova L, Soukup L, Jastrabik L, Chvostova D, Wagner T (2001) Surface and Coatings Technology **142–144**: 681
[15] Frait Z, Gemperle R (1971) Journ de Physique **32**: C1-541
[16] Frait Z, Fraitova D (1998) In: Wigen P, Baryachtar V, Lesnik N (eds) Frontiers in Magnetism of Reduced Dimension Systems, NATO ASI, Series 3, Kluver, Dordrecht, vol 49, pp 121–152
[17] Mitani S, Fujimori H, Ohnuma S (1997) J Magn Magn Mater **165**: 141
[18] Mitani S et al. (1999) J Magn Magn Mater **198, 199**: 179
[19] Sheng P, Abeles B, Arie Y (1973) Phys Rev Lett **31**: 44
[20] Altshuler BL, Aronov AG (1979) Sov Phys JETP **77**: 2028
[21] Inoue J, Maekawa S (1996) Phys Rev B **53**: R11927
[22] Mitani S, Takahashi S, Takanashi K, Yakushiji K, Maekawa S, Fujimori H (1998) Phys Rev Lett **81**: 2799

Received October 5, 2001. Accepted November 22, 2001